Electronic Supplementary Information

Exploring colorimetric-real time sensing behaviour of a newly designed CT complex toward nitrobenzene and Co^{2+}: Spectrophotometric, DFT/TD-DFT and mechanistic insights

Ishaat M. Khan*, Sonam Shakya
Department of Chemistry, Aligarh Muslim University, Aligarh 202002, India

Energy components of optimised CTC structure-

Wave-function normalization = 1.0000000000

One electron energy = -4838.1762948423
Two electron energy = 2057.8838655054
Nuclear repulsion energy = 1654.7549552613

Total energy = -1125.5374740755

Electron-electron potential energy = 2057.8838655054
Nucleus-electron potential energy = -5954.9935885800
Nucleus-nucleus potential energy = 1654.7549552613

Total potential energy = -2242.3547678133
Total kinetic energy = 1116.8172937377
Virial ratio (v/t) = 2.0078080635

Electrostatic moments -

Point 1	X	Y	Z (bohr)	charge
	10.092341	2.800889	12.964250	0.00 (a.u.)
	DX	DY	DZ	/D/ (DEBYE)
	-5.709808	2.564538	0.938024	6.329190

Table S1. Crystal data with refinement parameters for CTC.

Formula sum	**N4 C10 H8 O6**
Formula weight	**594.367 g/mol**
Temperature	RT
Wavelength	**0.71073 (Å)**
Crystal system	triclinic
Space-group	**P 1 (2)**
Cell Lengths	a=7.7171 Å b=12.0362 Å c=13.6112 Å
Cell Angles	a=97.7100° ß=101.9200° γ=92.3600°
Cell volume	**1222.73 Å^3**
Calc. density	0.459084 g/cm^3
Bond precision	C-C = 0.0046 A
Absorption coefficient	0.065
Theta range for data collection	2.26 to 28.46°
Reflections collected / unique	20895 / 7935 [R(int) = 0.1191]
Number of observed reflections [I>2σ(I)]	3580
Absorption correction	Empirical (SADABS)
Refinement method	Full-matrix least-squares on F^2
Goodness-of-fit on F^2	0.9810
Final R indices [I>2σ(I)]	R1=0.096 WR2 = 0.231
R indices (all data)	R1=0.200 WR2 = 0.317
Largest diff. peak and hole	0.7700, -0.7000 e.Å^{-3}

Table S2. Weight loss, enthalpy (ΔH), and degradation temperature (T), for pyrazole, 3,5-dinitrobenzoic acid and PYR: DNB CT complex.

Step	Imidazole			Picric acid			CTC $[(IMH)^{+}(PA)^{-}]$		
	Weight loss (%)	T(^{0}C)	ΔH(mJ)	Weight loss (%)	T(^{0}C)	ΔH(mJ)	Weight loss (%)	T(^{0}C)	ΔH(mJ)
1	99.92	199.93	-371.74	99.26	274.44	-276.04	81.98	314.27	-189.10
2			-526.18			-430.63			-176.82
3									-354.00

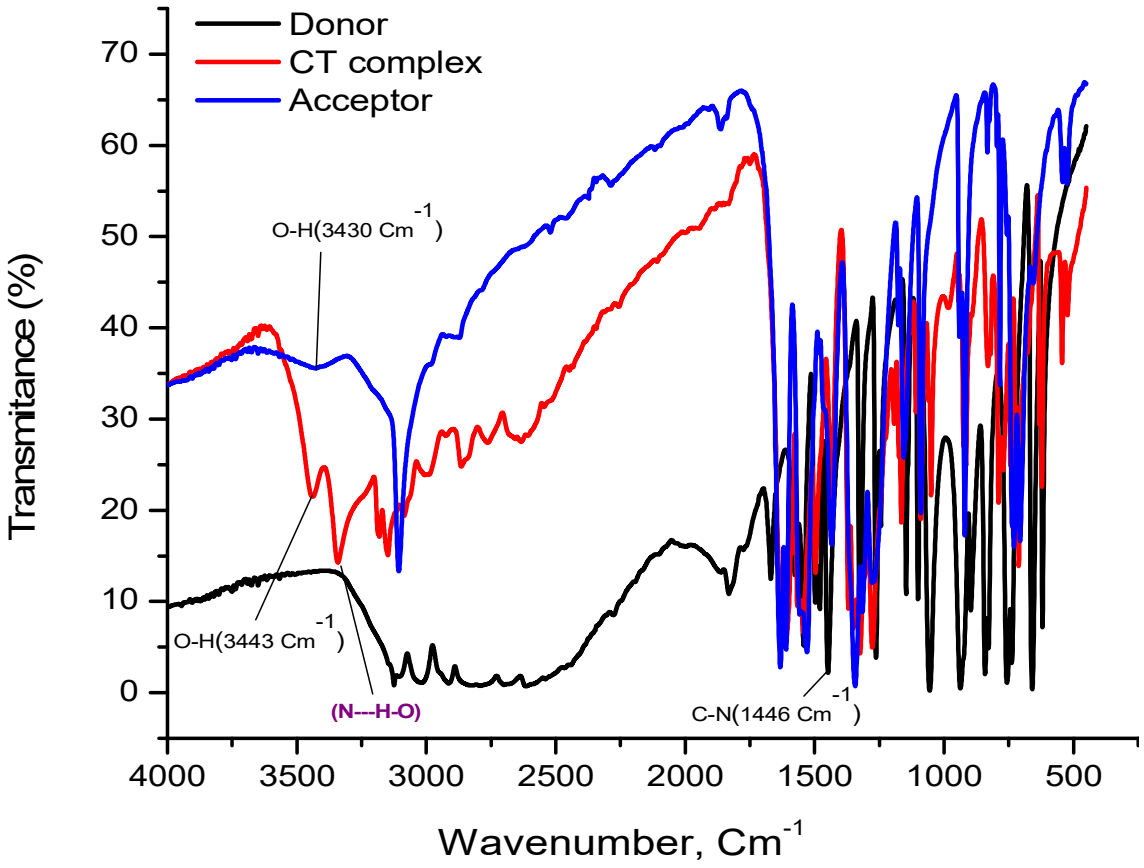

Figure S1. FTIR spectra of PA (top), charge transfer complex (middle) and IM (bottom).

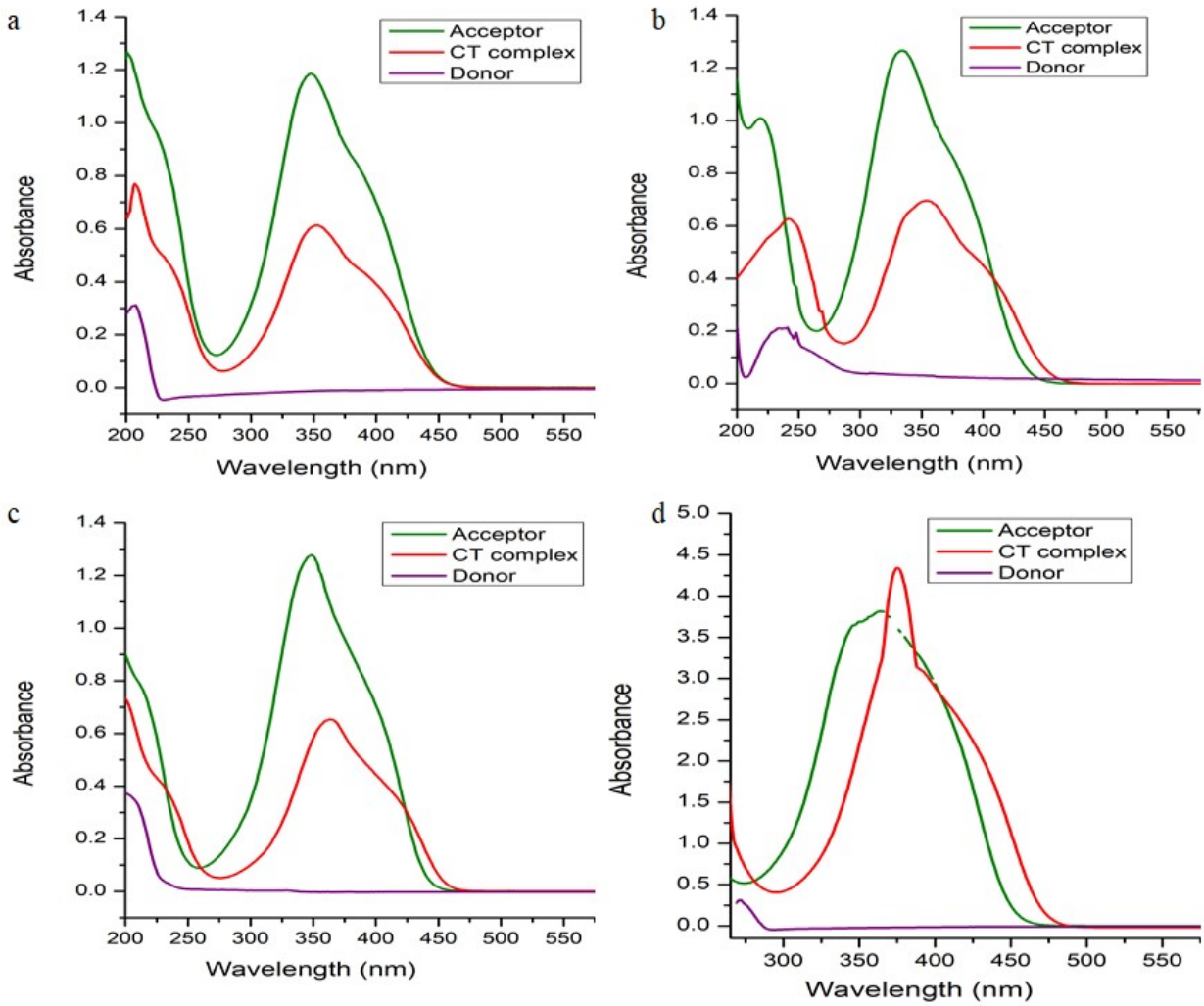

Figure S2. Electronic absorption spectra of acceptor (1×10^{-4} M), CT complex (1×10^{-4} M + 1×10^{-4} M) and donor (1×10^{-4} M) in (a) ethanol, (b) methanol, (c) acetonitrile and (d) DMSO/H_2O at room temperature.

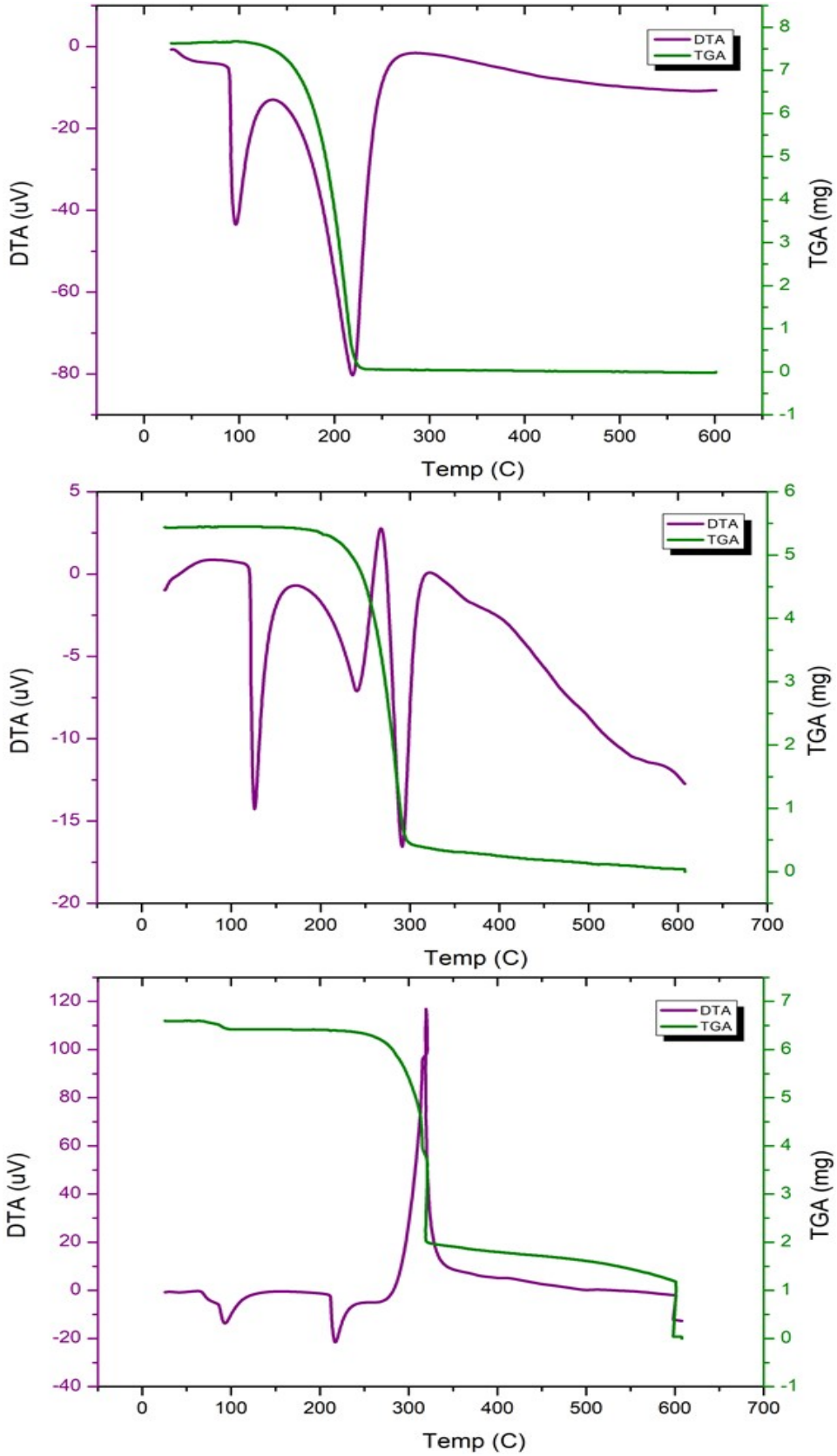

Figure S3. TGA–DTA curves for (Top) IM, (middle) PA and (bottom) CTC.

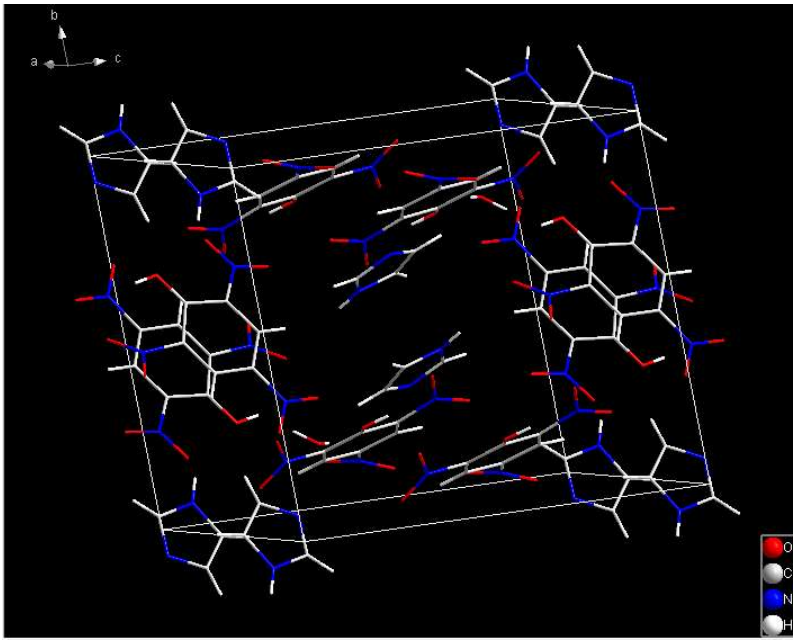

Figure S4. Crystal packing of the synthesised CTC obtained through SC-XRD.

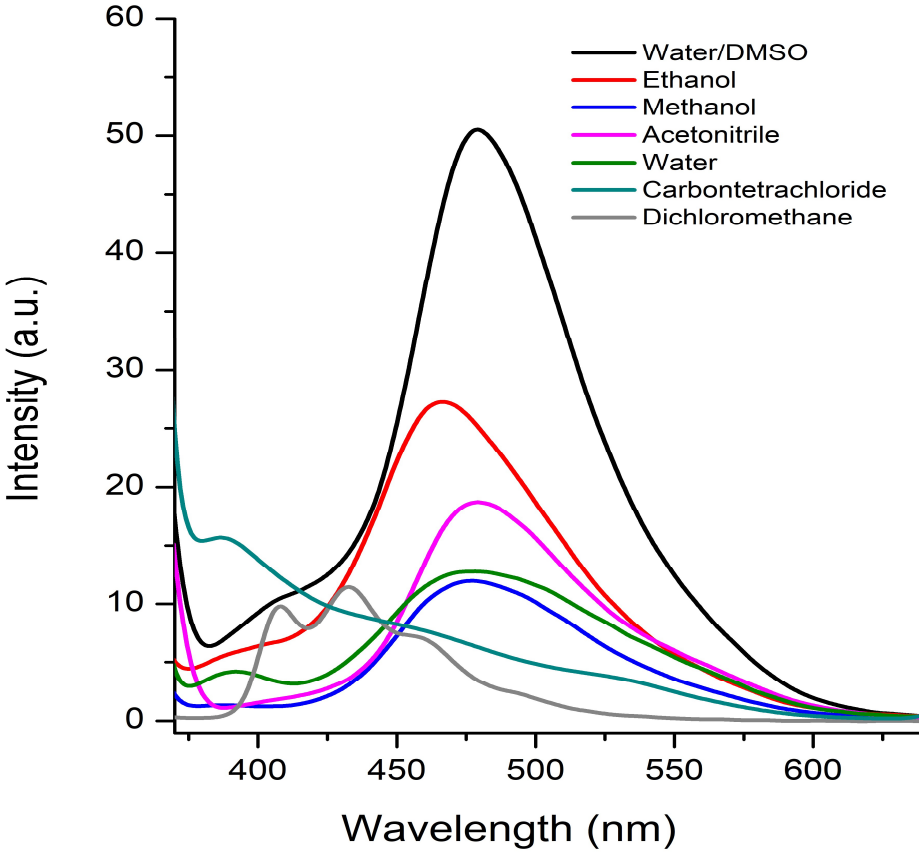

Figure S5. Emission spectra of CTC dispersed in different solvents upon excitation at 340 nm.

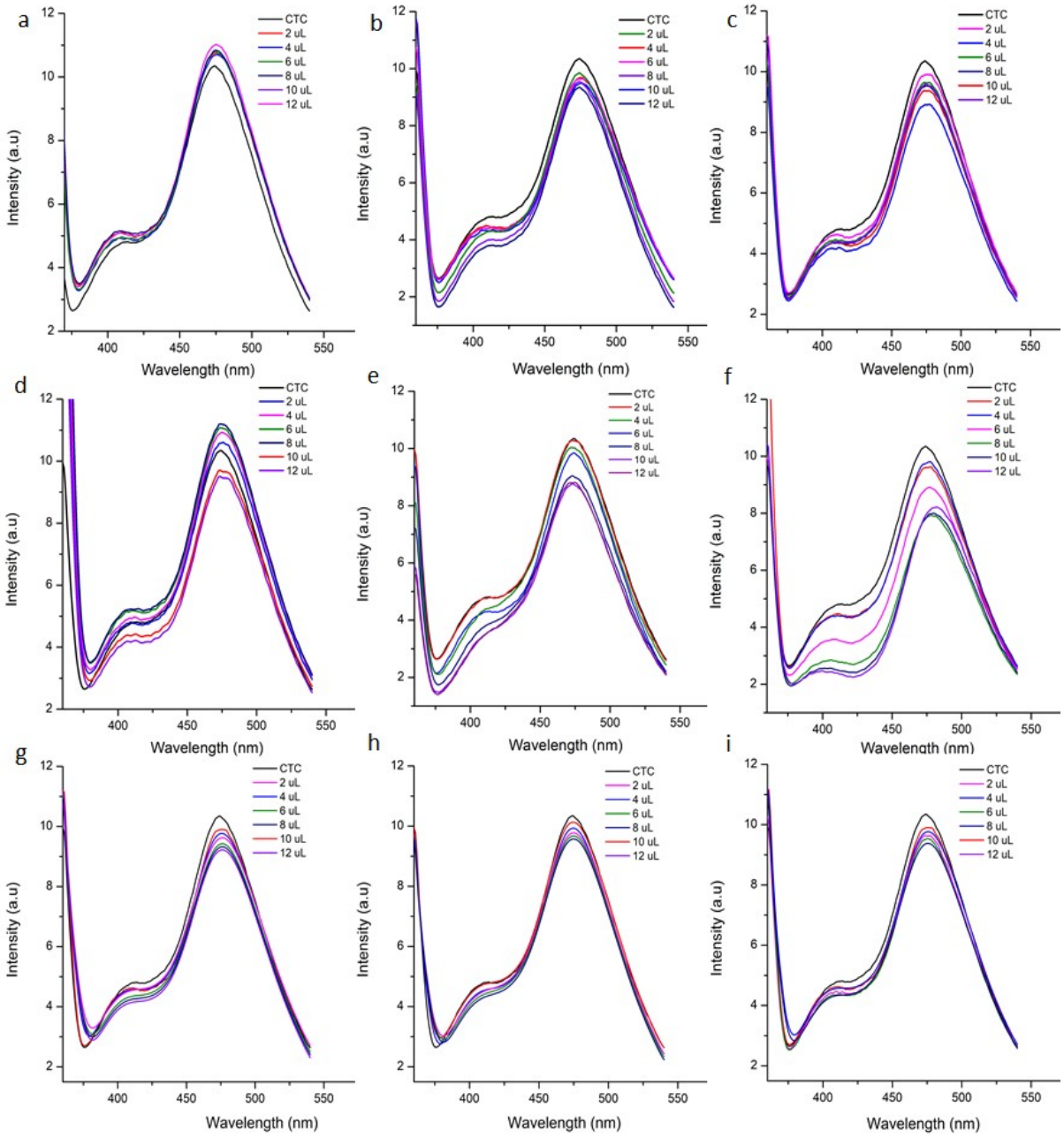

Figure S6. The change in fluorescence intensity of CTC upon incremental addition of (a) TNP, (b) DNB, (c) DNP, (d) MNA, (e) ONP, (f) ONA, (g) DNT, (h) NT and (i) p-DNB.

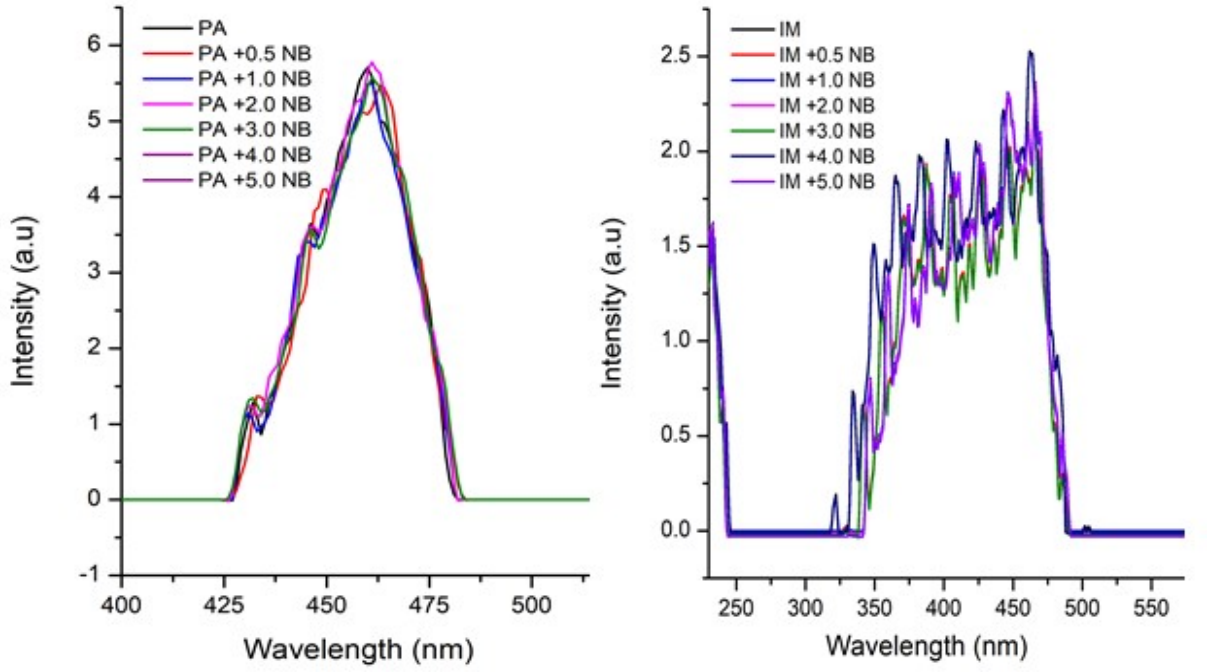

Figure S7. The change in fluorescence intensity of PA (left) and IM (right) on adding NB.

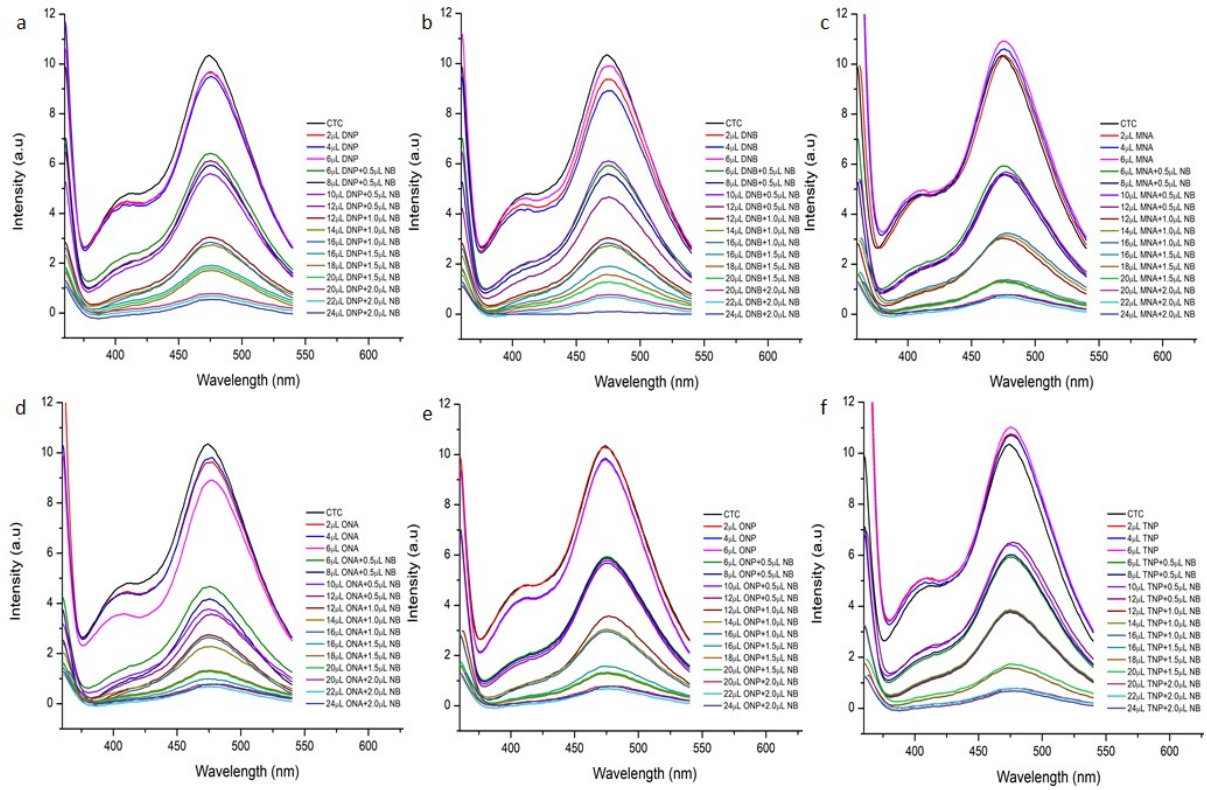

Figure S8.The change in fluorescence intensity of CTC upon addition of different nitro analytes (a) DNP, (b) DNB, (c) MNA, (d) ONA, (e) ONP and (f) TNP followed by NB.

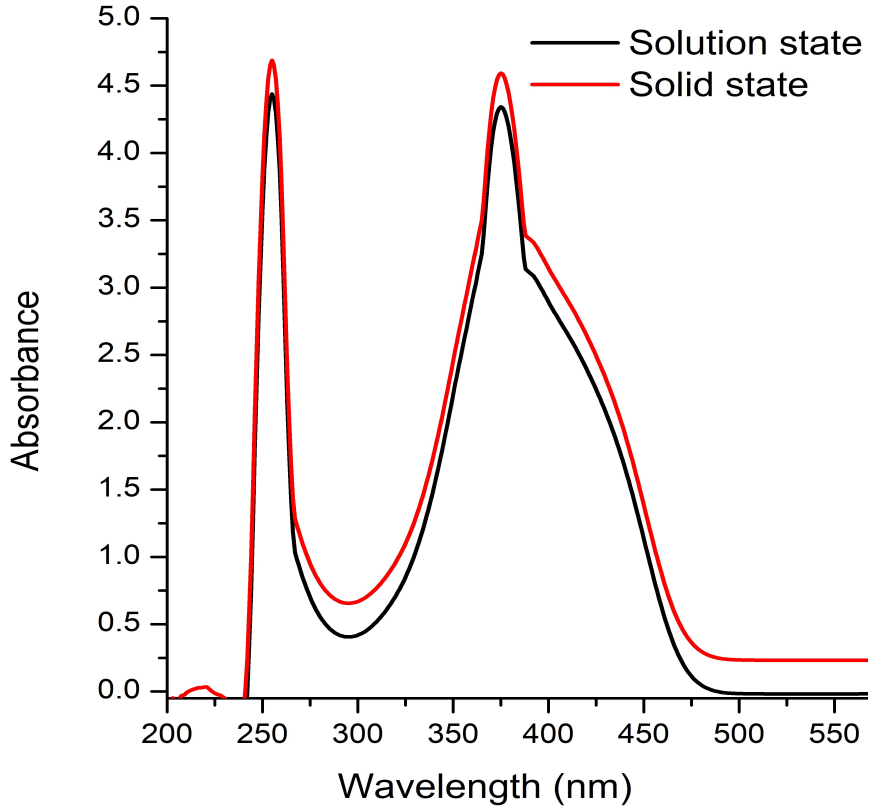

Figure S9. Solution and solid state UV-vis spectra of CTC.

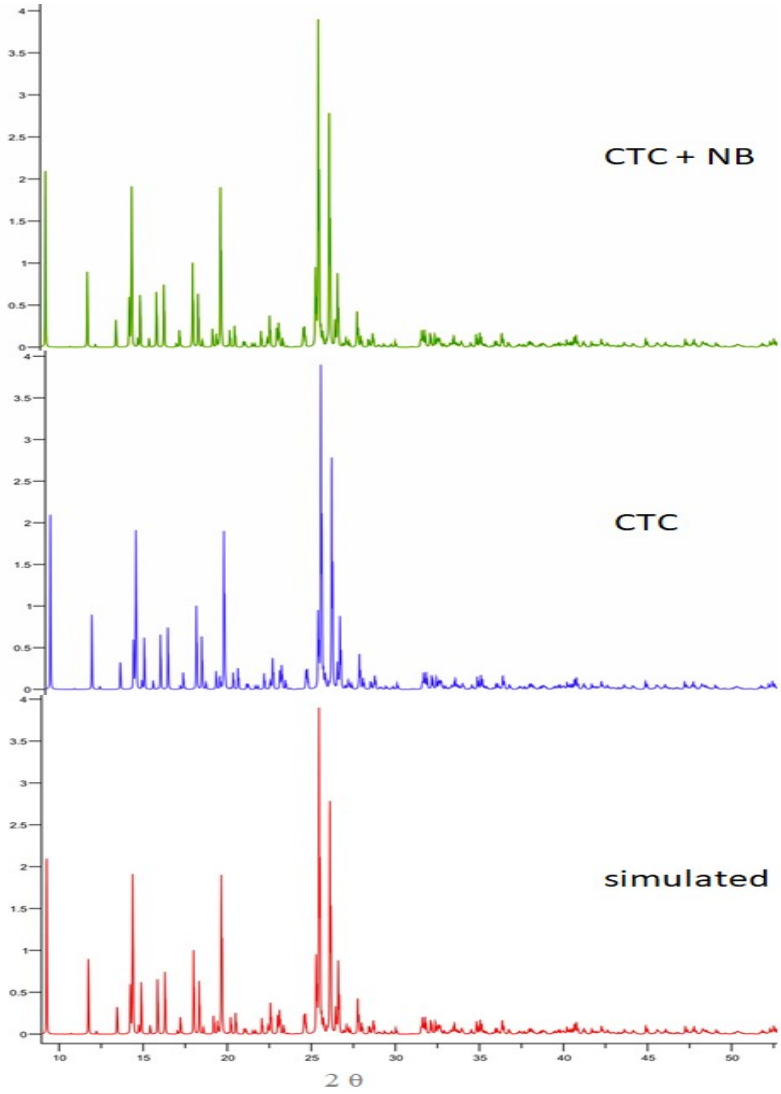

Figure S10. Powder XRD patterns of CTC+NB (top), CTC (middle) and simulated (bottom).

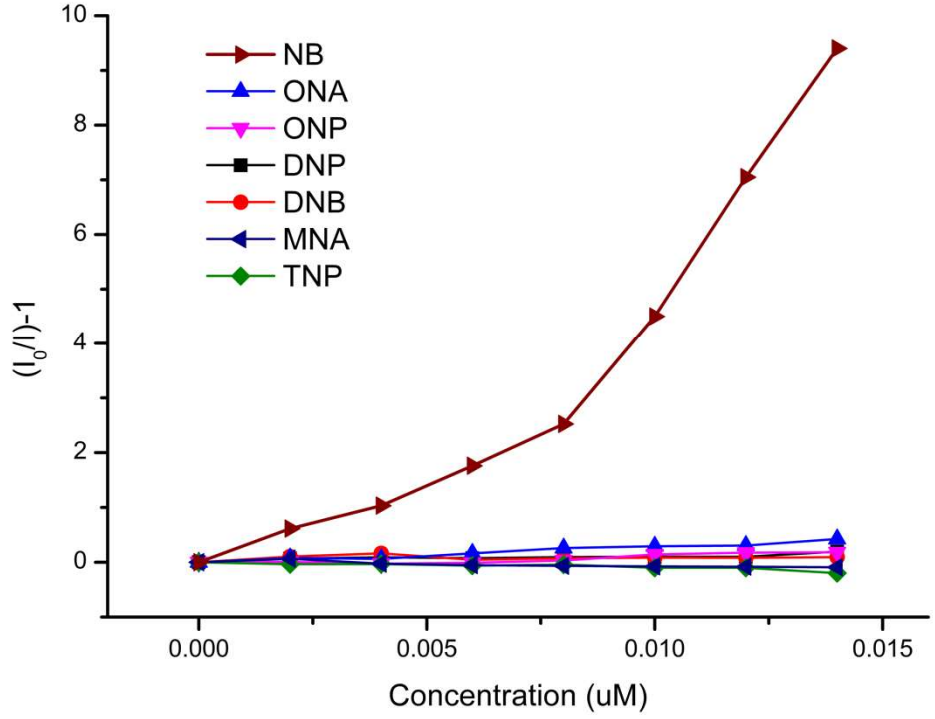

Figure S11. Stern-Volmer (SV) plots for various nitro analytes in DMSO/H_2O.

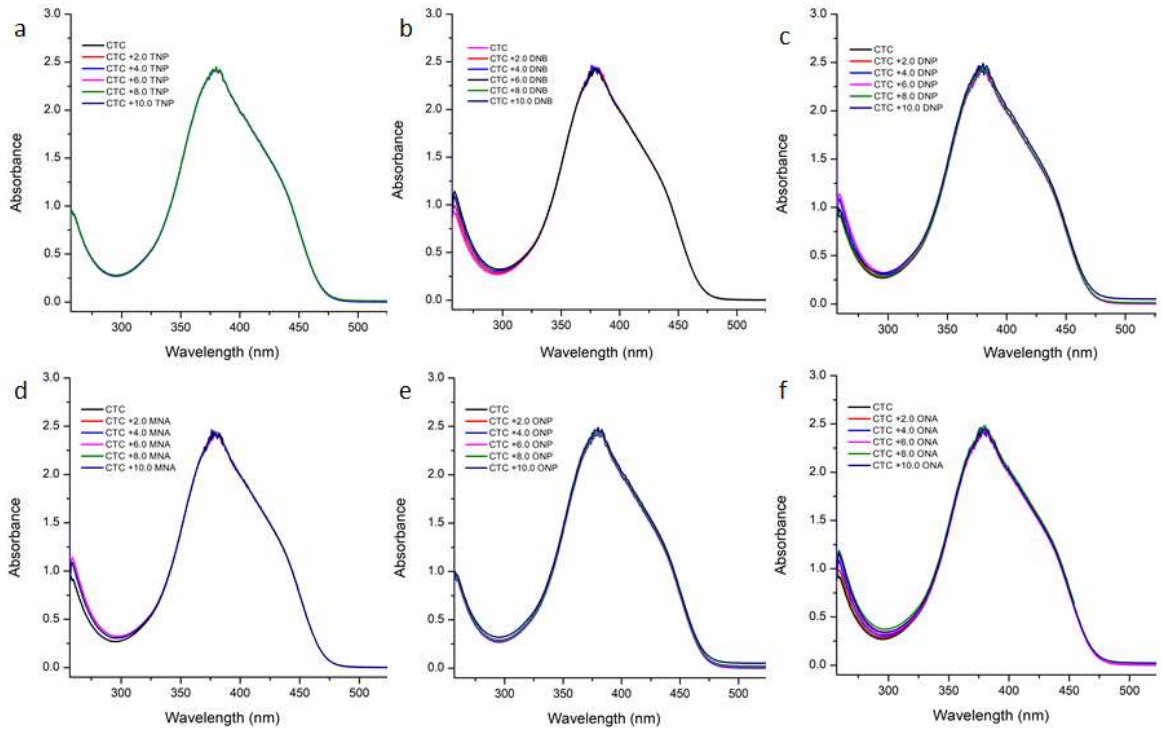

Figure S12.UV- vis spectra of CTC upon incremental addition of (a) TNP, (b) DNB, (c) DNP, (d) MNA, (e) ONP and (f) ONA.

Table S3. HOMO and LUMO energies calculated for nitro-analytes and ligand at B3LYP/6-31G* level of theory.

Analytes	HOMO (eV)	LUMO (eV)	Band gap (eV)
DNB	-8.244	-3.724	4.520
ONP	-9.877	1.150	8.050
ONA	-0.6133	-0.803	0.191
MNA	-6.501	-2.896	3.611
DNP	-6.311	-3.611	2.621
TNP	-8.37	-4.566	3.806
NB	-7.636	-3.149	4.487
CTC	-6.911	-3.005	4.010

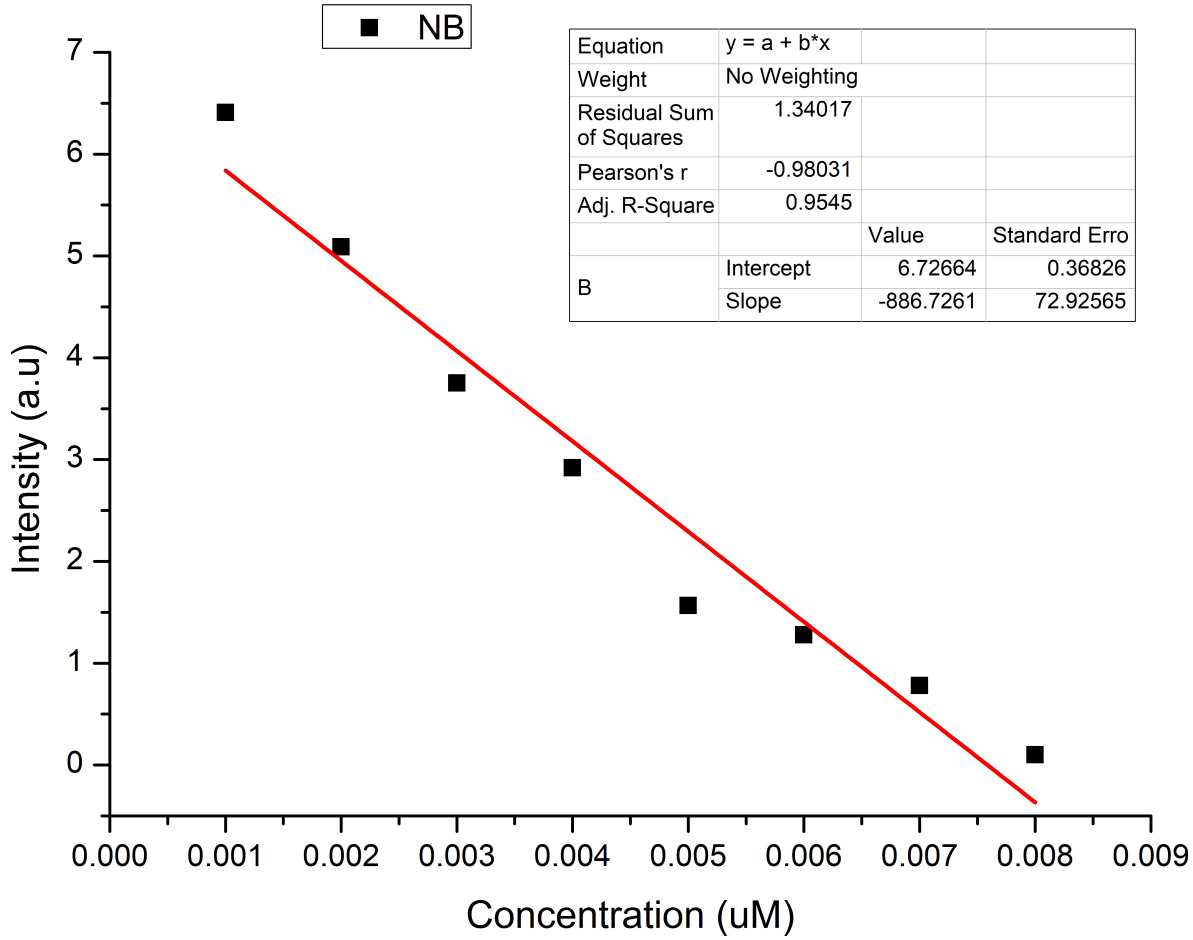

Figure S13. Linear region of fluorescence intensity of CTC upon addition of NB (0.5 – 5 µL, 1 mM stock solution) in water/DMSO.

Table S4. Calculation of standard deviation for CTC.

Blank Readings (only probe)	FL Intensity of CTC
Reading 1	10.35
Reading 2	10.98
Reading 3	11.58
Reading 4	10.01
Reading 5	11.99
Standard Deviation(σ)	**0.8242997**

Table S5. Detection limit calculation of CTC for NB.

Complex	Slope from Graph (m)	Detection limit ($3\sigma/m$)	
		μM	ppb
CTC	886.726	2.788 E-03	~0.114

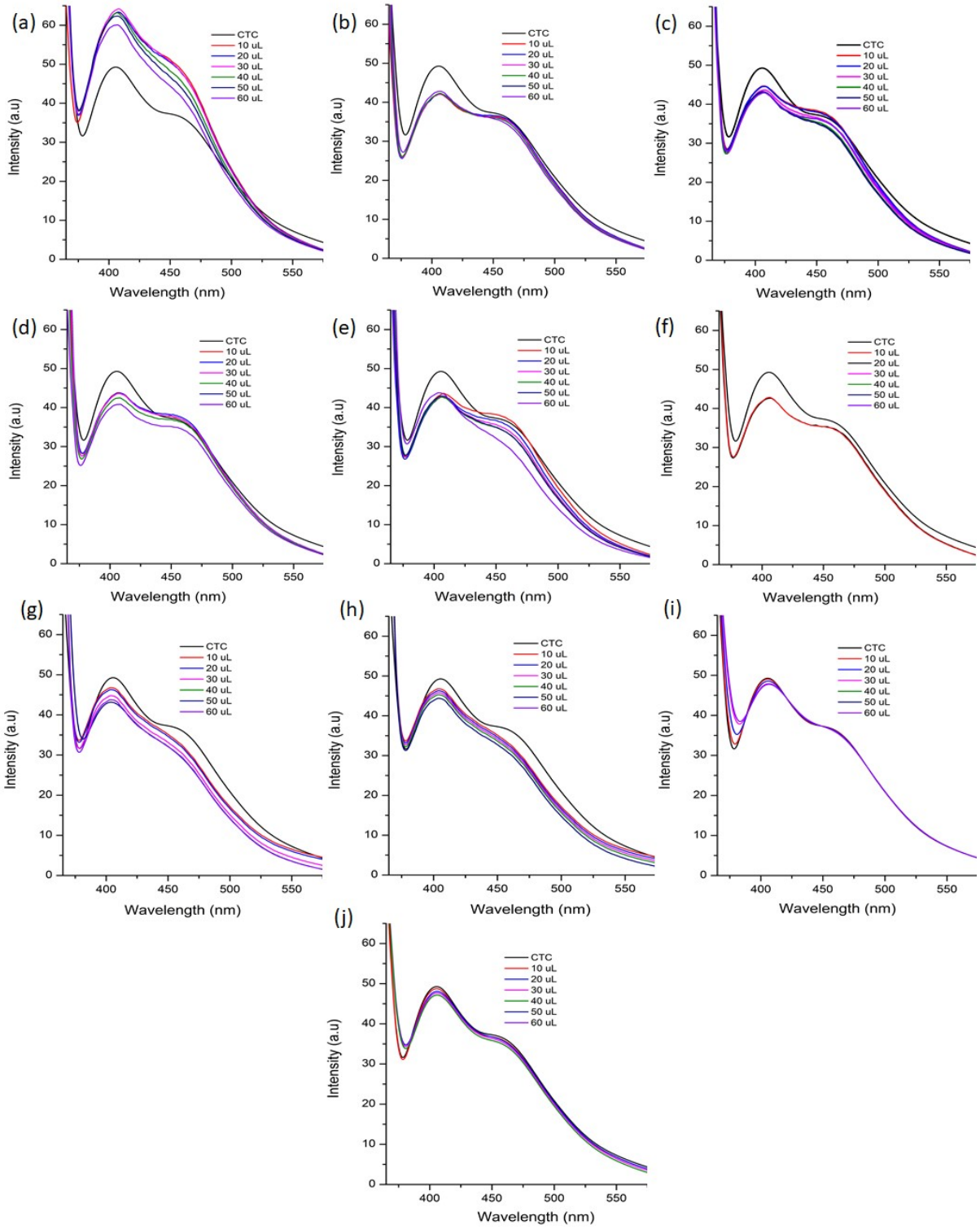

Figure S14. The change in fluorescence intensity of CTC upon incremental addition of (a) Cr^{2+}, (b) Mn^{2+}, (c) Ni^{2+}, (d) Zn^{2+}, (e) Cu^{2+}, (f) Fe^{2+}, (g) Ca^{2+}, (h) Li^{+}, (i) Na^{+} and (j) K^{+}.

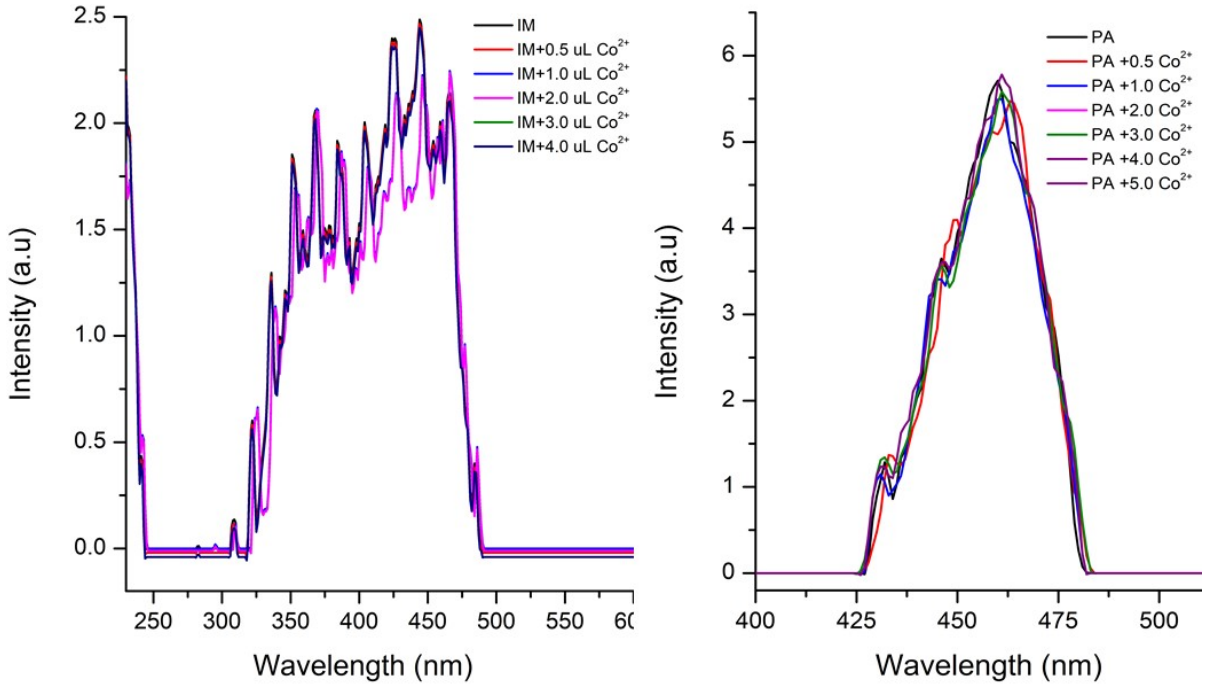

Figure S15. The change in fluorescence intensity of PA (left) and IM (right) on adding Co^{2+}.

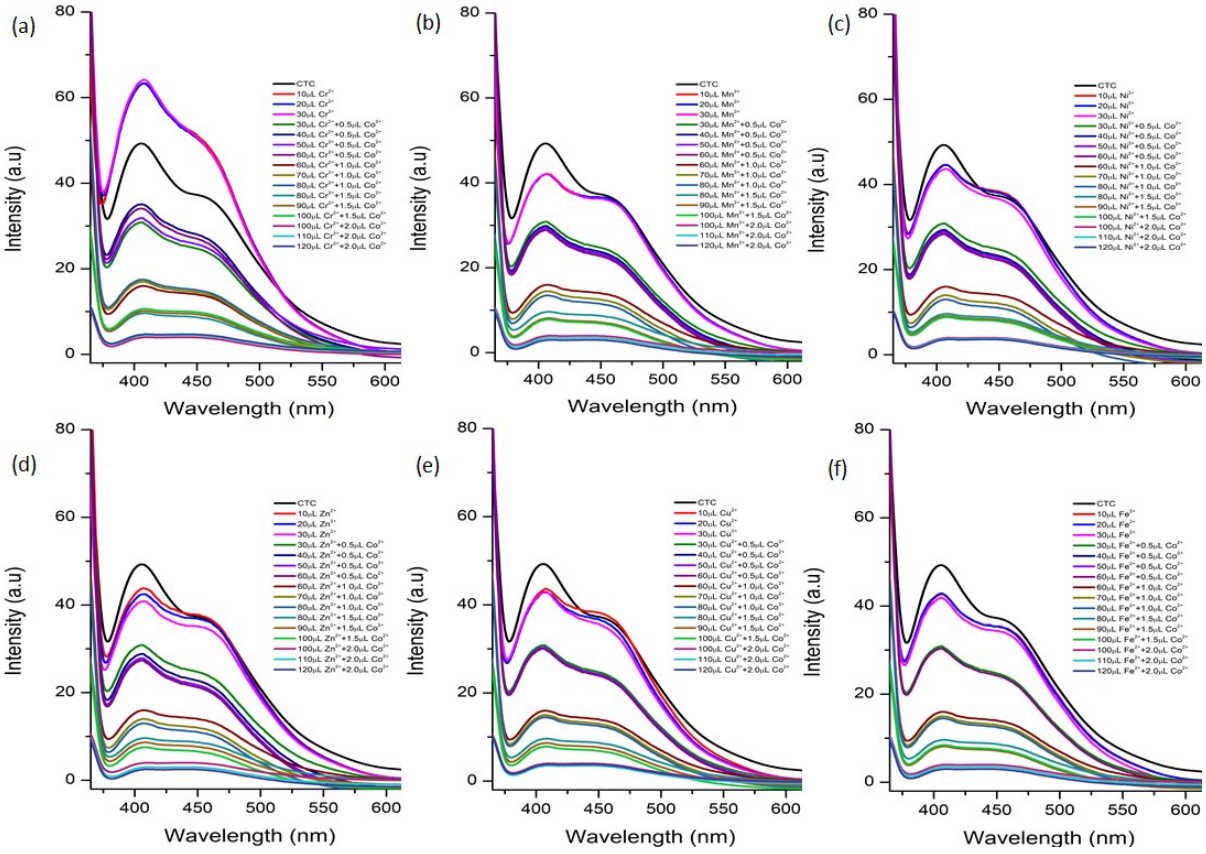

Figure S16. The change in fluorescence intensity of CTC upon addition of different metal ions followed by Co^{2+}.

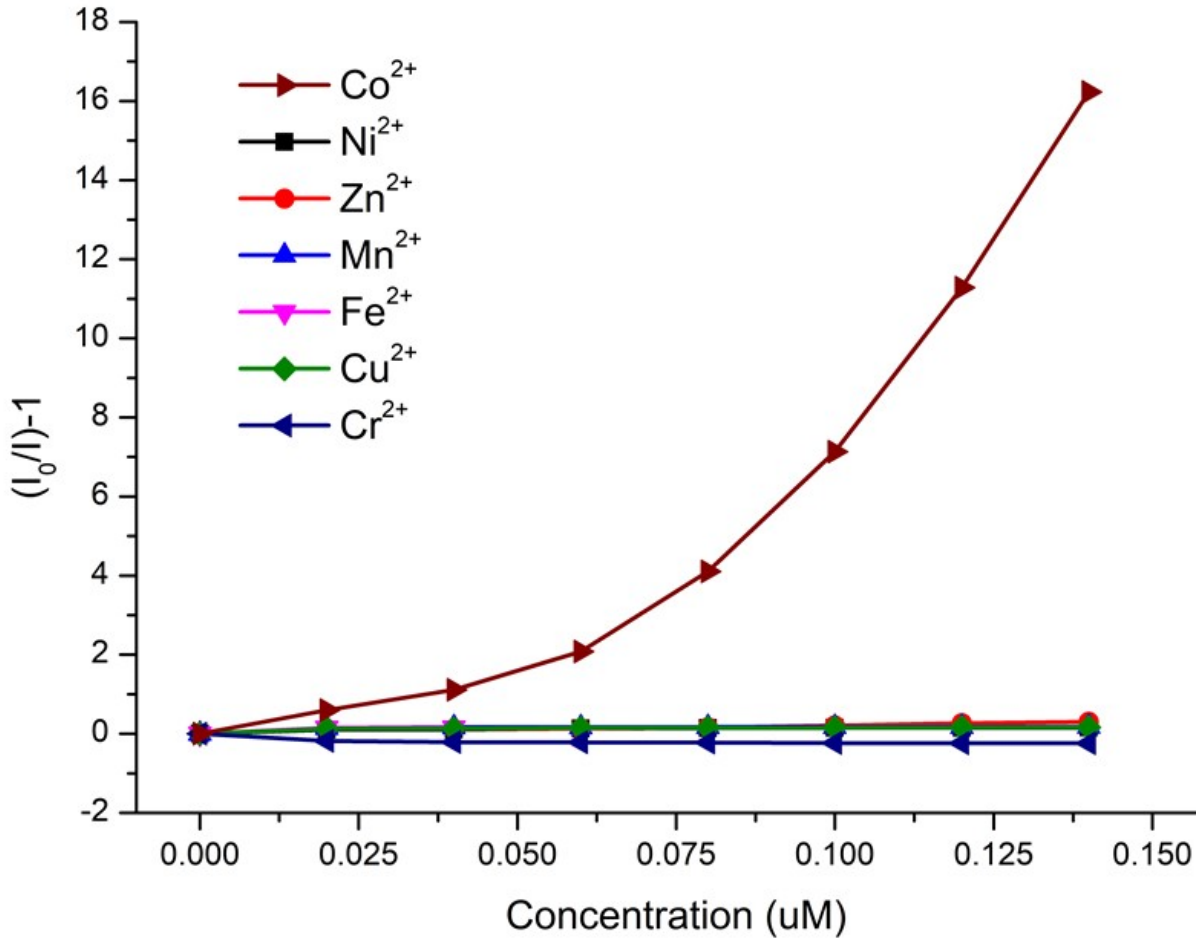

Figure S17. Stern-Volmer (SV) plots for various metal ions in DMSO/H_2O.

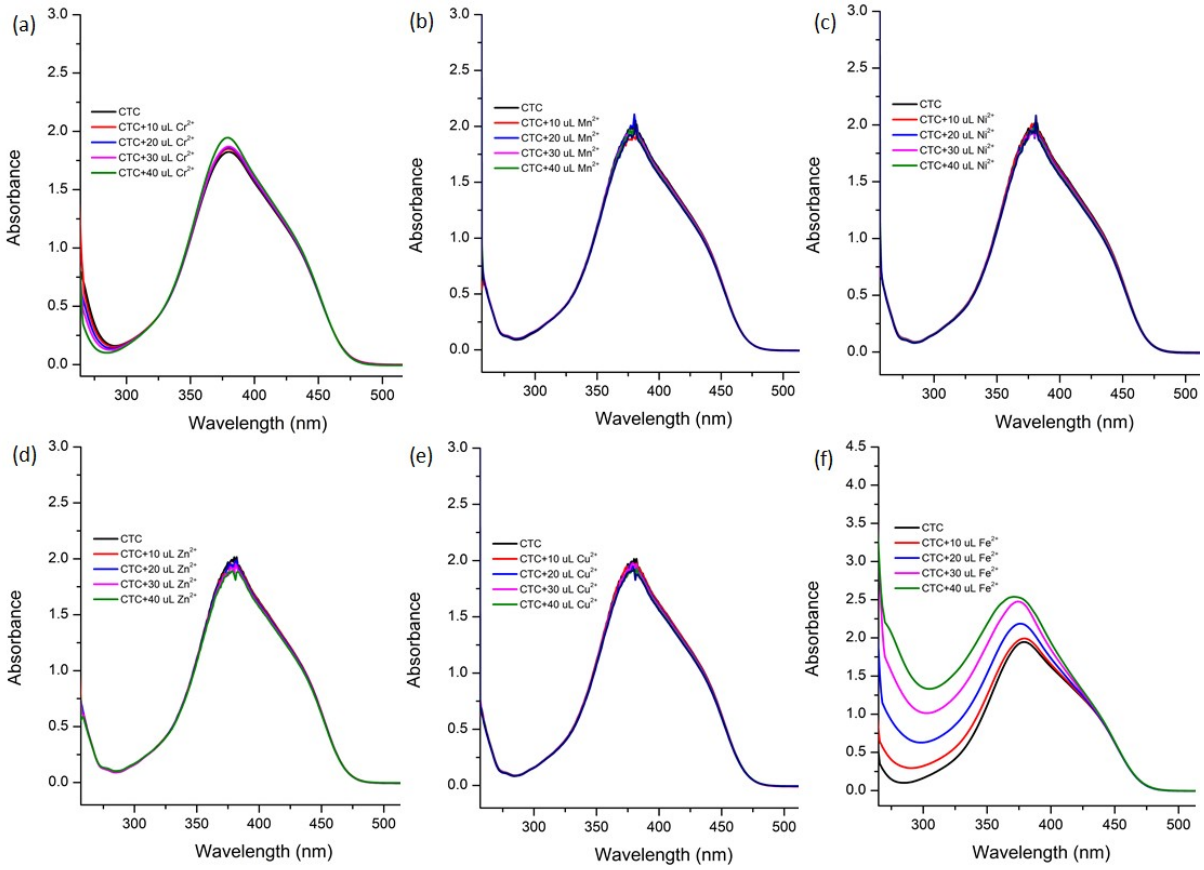

Figure S18. UV-vis spectra of CTC upon incremental addition of (a) Cr^{2+}, (b) Mn^{2+},(c) Ni^{2+}, (d) Zn^{2+}, (e) $Cu^{2+}$and (f) Fe^{2+}.

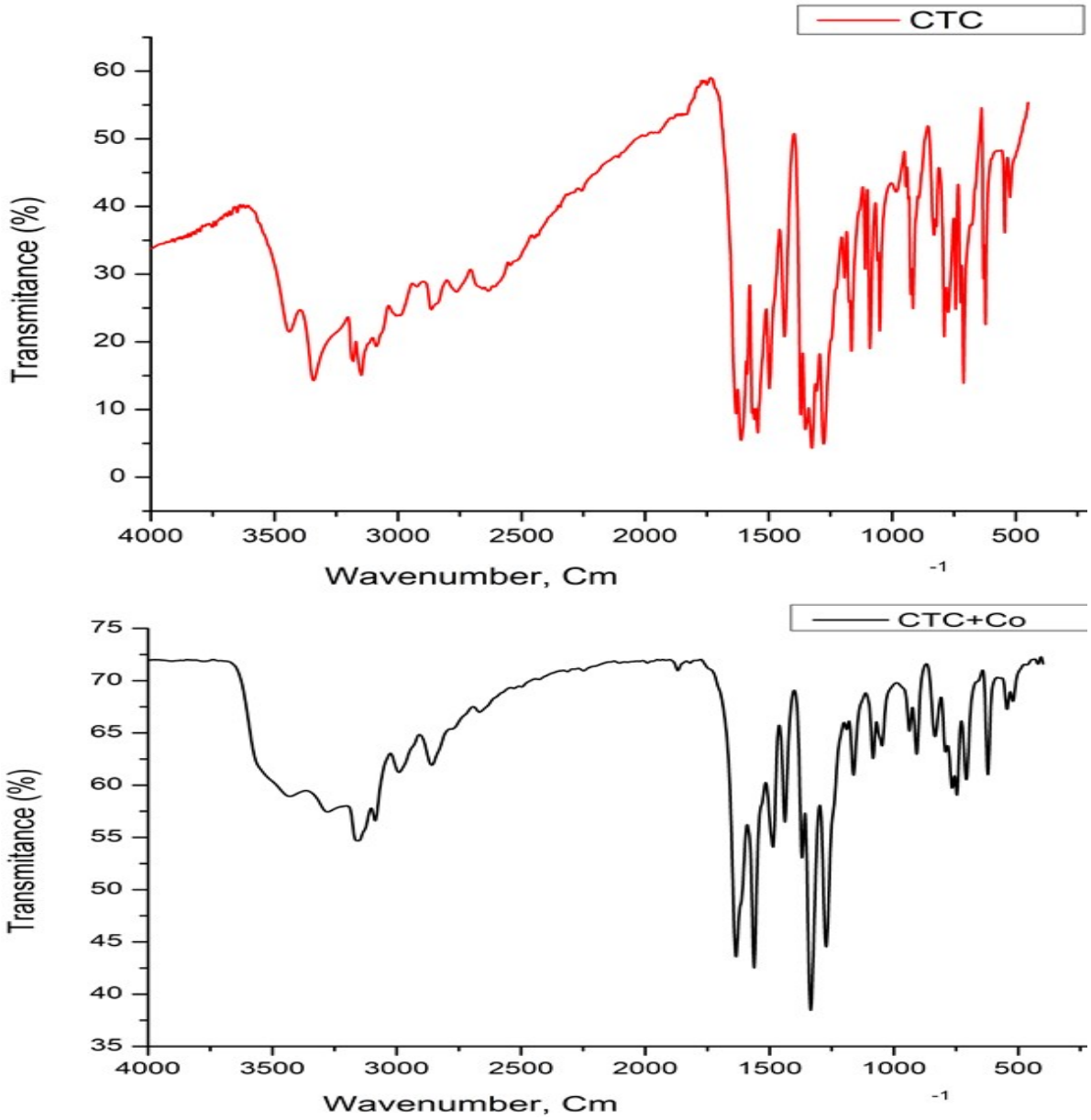

Figure S19. FTIR of CTC (top) and CTC-Co^{2+} (bottom).

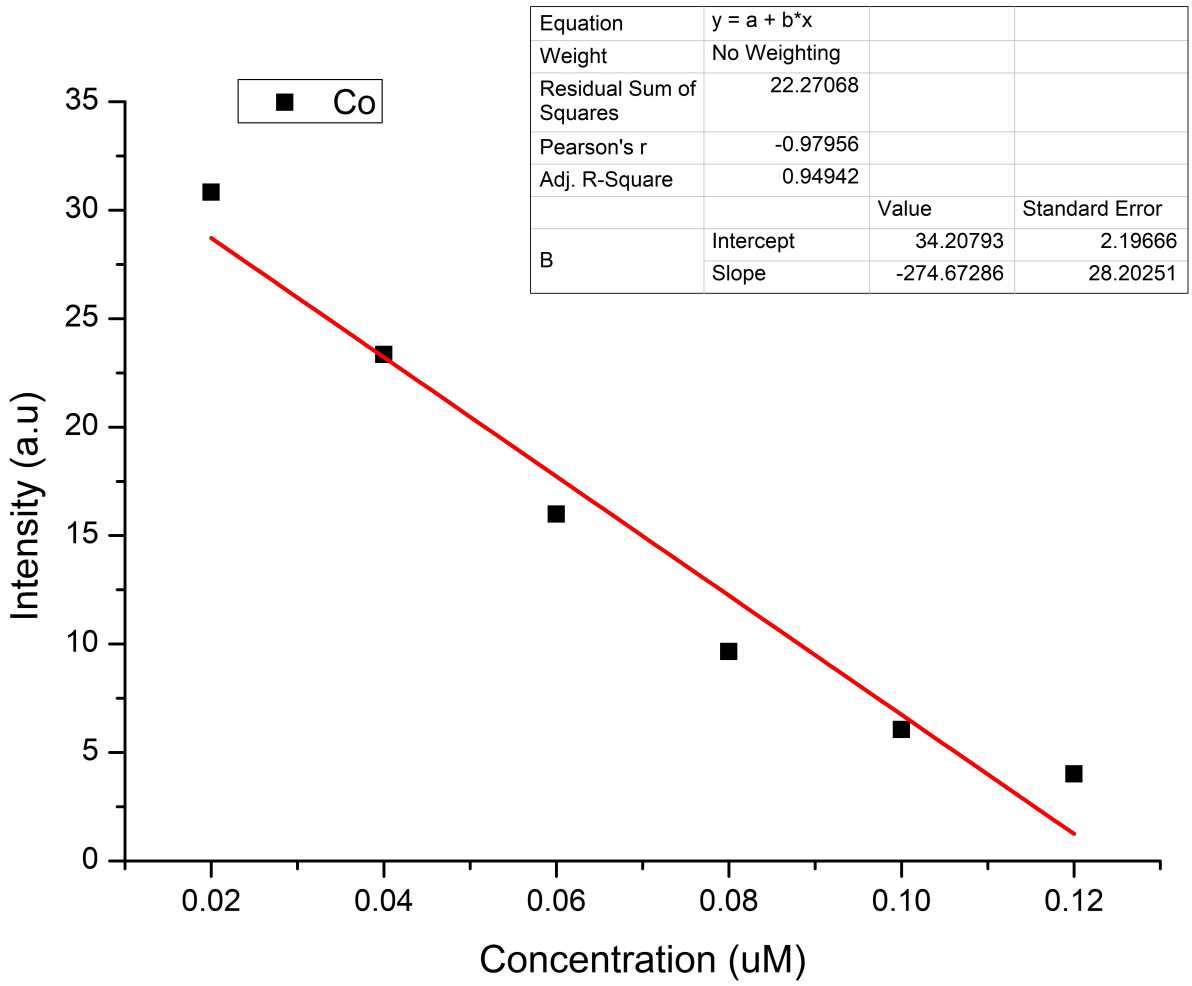

Figure S20. Linear region of fluorescence intensity of CTC upon addition of NB (0.5 – 5 µL, 1 mM stock solution) in water/DMSO.

Table S6. Calculation of standard deviation for CTC

Blank Readings (only probe)	FL Intensity of CTC
Reading 1	49.26
Reading 2	51.22
Reading 3	50.00
Reading 4	49.98
Reading 5	49.99
Standard Deviation (σ)	**0.7033850**

Table S7. Detection limit calculation of CTC for NB.

Complex	Slope from Graph (m)	Detection limit ($3\sigma/m$)	
		µM	ppb
CTC	274.672	7.684 E-03	~0.589

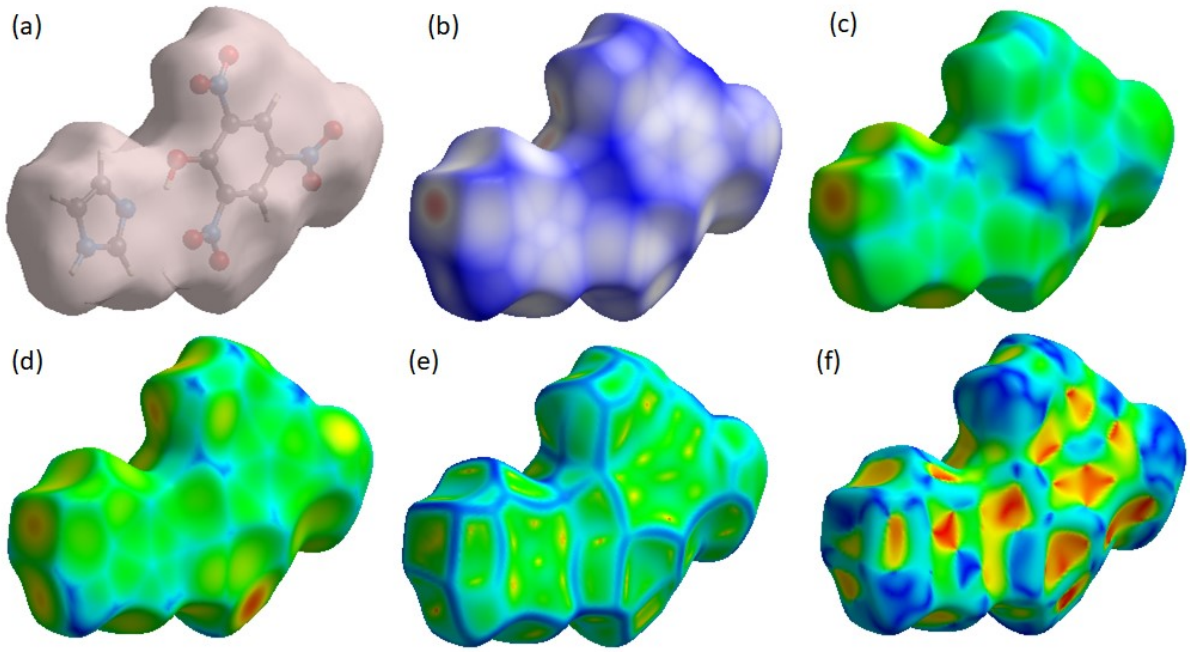

Figure S21. Hirshfeld surface of the CTC mapped with (a) none, (b) d_{norm}, (c) d_i, (d) d_e, (e) curvedness, (f) shape index.

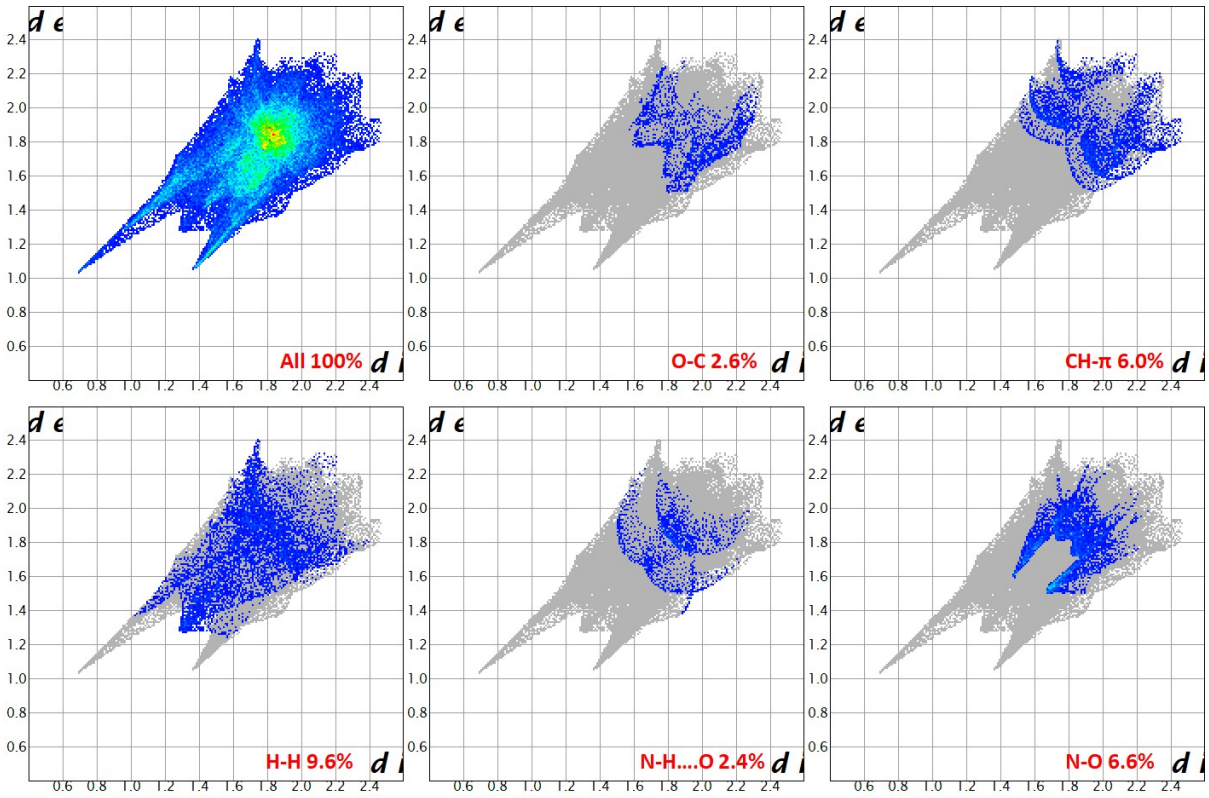

Figure S22. 2D fingerprint plots of the CT complex representing different intermolecular interactions.

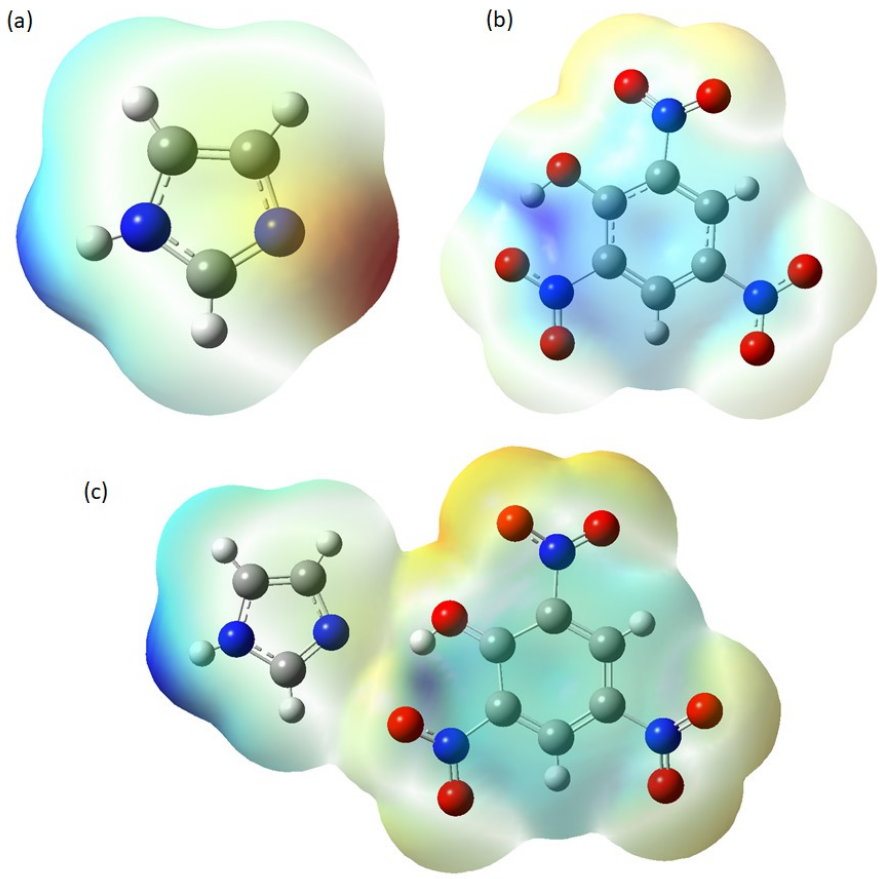

Figure S23. MEP surface map of (a) IM, (b) PA and (c) CTC showing difference in colour.

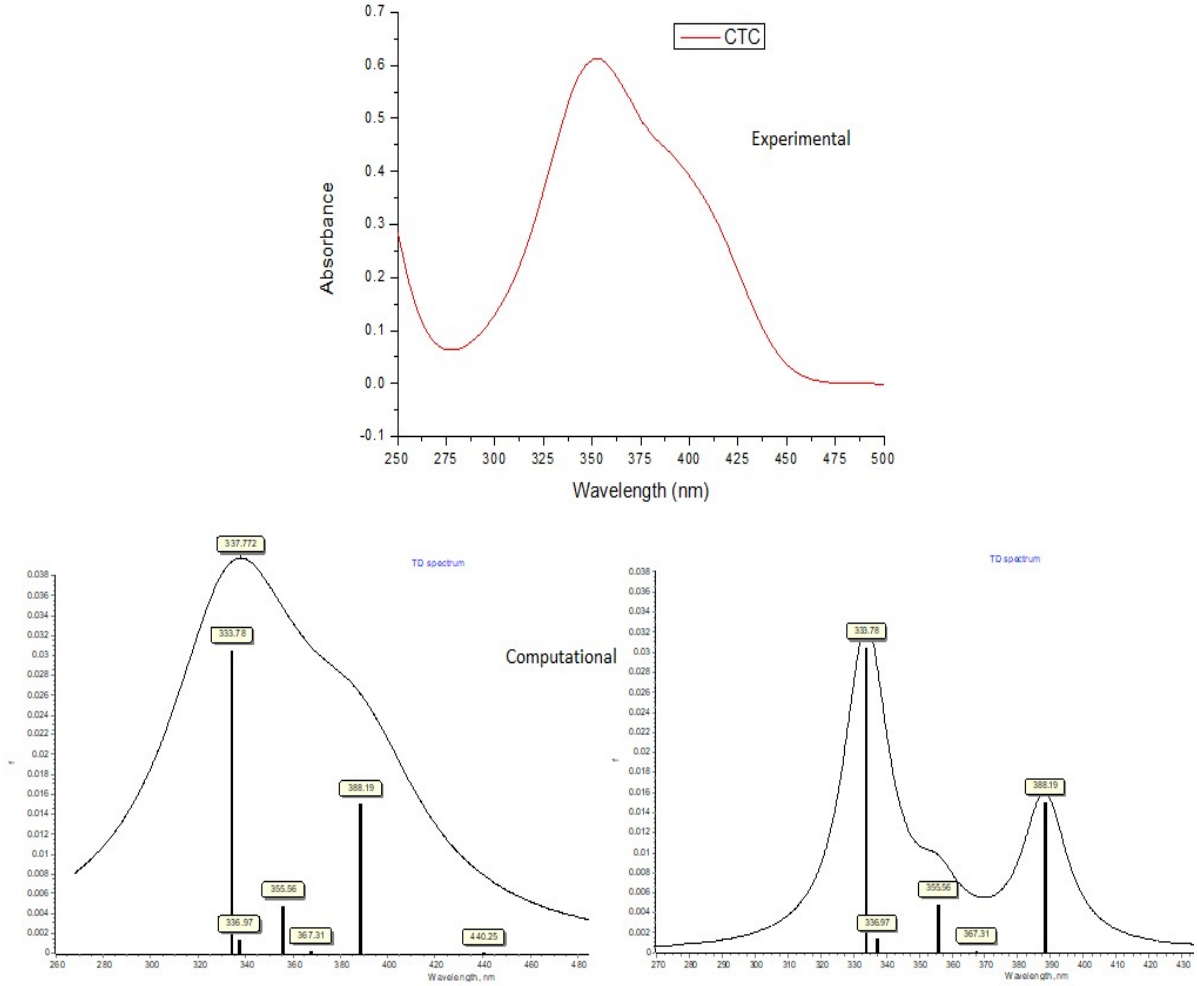

Figure S24. Experimental (top) and Computational by TD-DFT (bottom) UV-vis spectra of CTC.

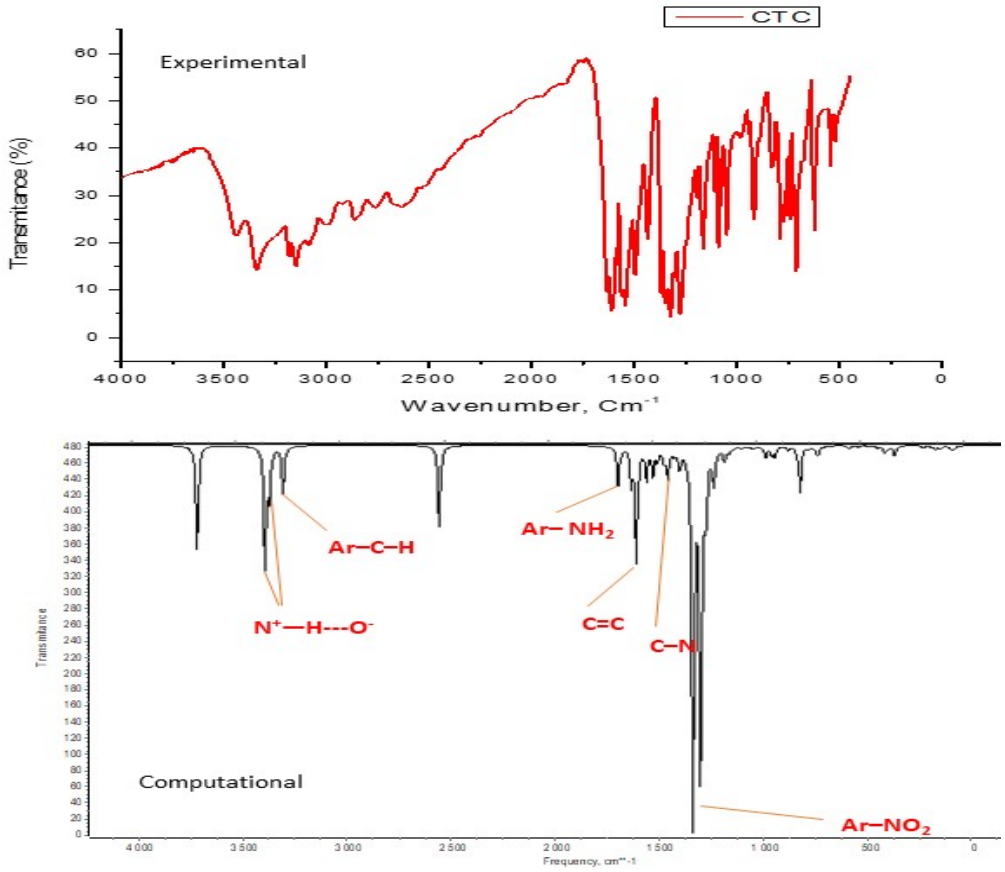

Figure S25. Experimental (top) and Computational by TD-DFT (bottom) FTIR spectra of CTC.

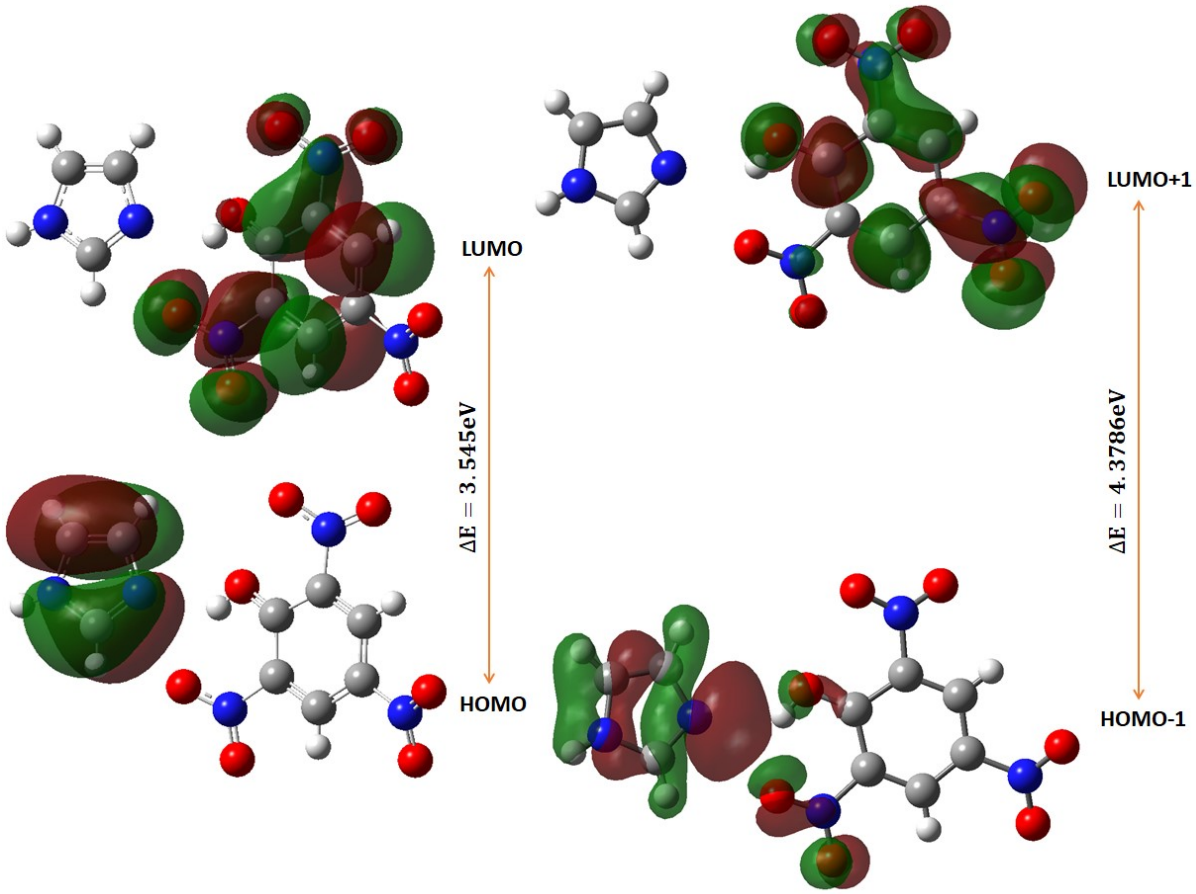

Figure S26. The pictorial representation of frontiers molecular orbital.

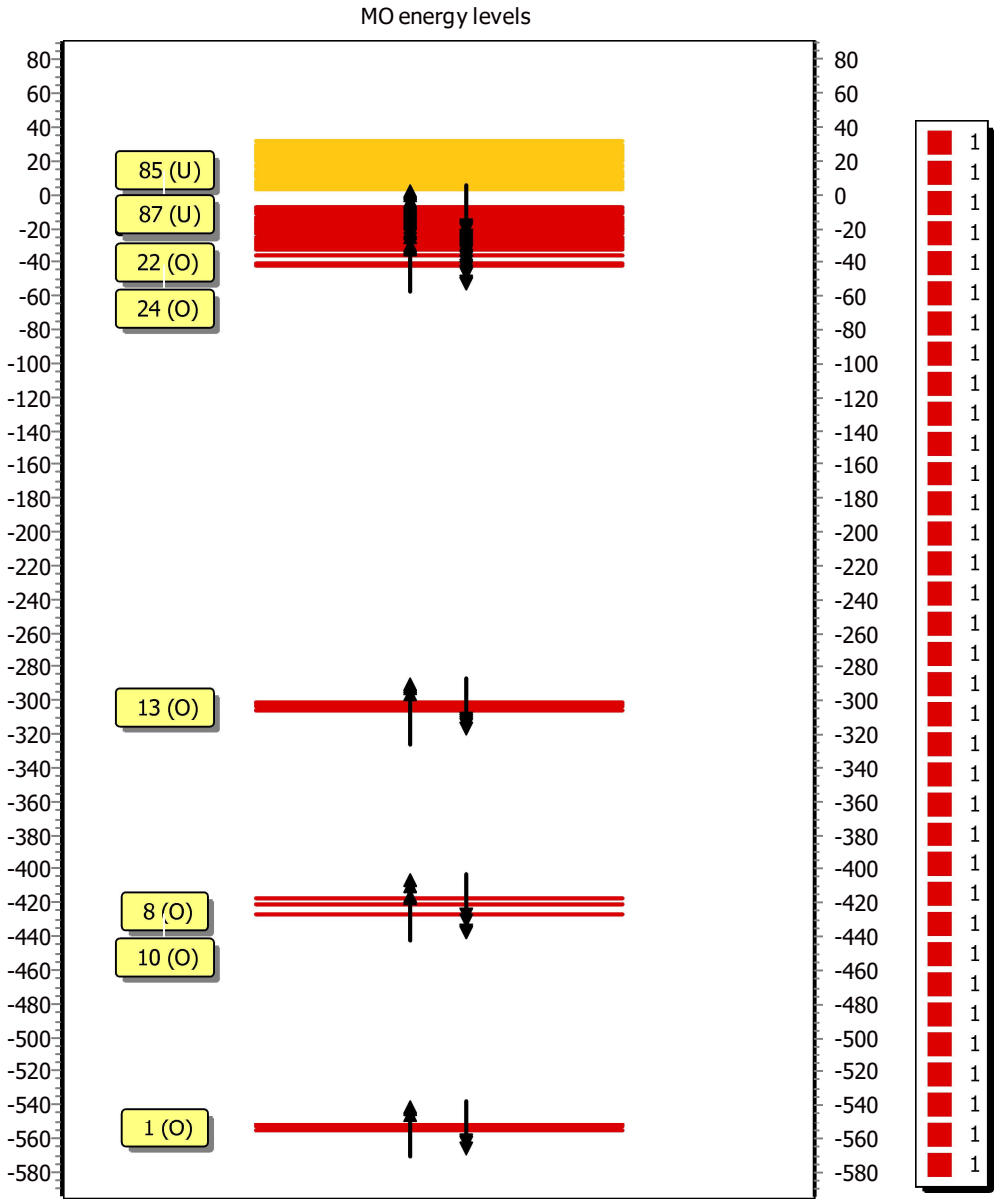

Figure S27. MO energy level diagram of CTC.

Table S8. Molecular orbital energies for CT complex.

MO NO.	Energy	MO NO.	Energy	MO NO.	Energy
1	-555.43	37	-25.3095	73	-8.30498
2	-552.175	38	-22.9884	74	-8.08729
3	-551.963	39	-22.3679	75	-7.97572
4	-551.821	40	-21.7285	76	-7.79884
5	-551.77	41	-21.0835	77	3.63547
6	-551.541	42	-20.9475	78	4.079019
7	-551.155	43	-20.7244	79	5.393339
8	-426.945	44	-19.6141	80	7.129439
9	-426.64	45	-18.9447	81	7.368901
10	-426.637	46	-18.6916	82	7.534892
11	-420.661	47	-18.5937	83	10.1717
12	-417.08	48	-18.3733	84	11.39622
13	-305.739	49	-18.0685	85	12.13365
14	-303.271	50	-17.9678	86	13.77179
15	-303.178	51	-17.4127	87	14.20446
16	-303.154	52	-16.8467	88	15.91879
17	-303.096	53	-16.6372	89	16.58275
18	-303.045	54	-16.4385	90	17.73108
19	-302.446	55	-16.3841	91	17.96782
20	-301.578	56	-16.2263	92	19.45629
21	-300.745	57	-15.9079	93	19.67127
22	-42.2487	58	-15.8154	94	19.8563
23	-42.0827	59	-15.5487	95	19.94066
24	-41.8977	60	-15.282	96	20.57741
25	-40.7113	61	-14.0874	97	20.67265
26	-36.0336	62	-13.5378	98	21.06722
27	-35.9656	63	-10.6044	99	21.60873
28	-35.7533	64	-10.5744	100	22.4659
29	-35.5737	65	-10.2833	101	22.66182
30	-32.5287	66	-10.0792	102	23.21149
31	-31.3069	67	-10.0003	103	24.53942
32	-29.911	68	-9.92679	104	24.92855
33	-29.3232	69	-9.78801	105	25.11631
34	-27.2878	70	-9.76624	106	25.49727
35	-25.9762	71	-9.60025	107	25.95442
36	-25.5762	72	-8.37845	108	26.74084